EXAFS study of the local structure of InAs up to 80 GPa

2005 J. Phys.: Condens. Matter 17 1811

(http://iopscience.iop.org/0953-8984/17/12/005)

INSTITUTE OF PHYSICS PUBLISHING JOURNAL OF PHYSICS: CONDENSED MATTER

J. Phys.: Condens. Matter **17** (2005) 1811–1824 doi:10.1088/0953-8984/17/12/005

EXAFS study of the local structure of InAs up to 80 GPa

Giuliana Aquilanti[1] **and Sakura Pascarelli**

European Synchrotron Radiation Facility, 6 rue Jules Horowitz, BP 220, Grenoble Cedex 09, 38043, France

E-mail: aquilanti@esrf.fr

Received 24 November 2004, in final form 18 February 2005
Published 11 March 2005
Online at stacks.iop.org/JPhysCM/17/1811

Abstract

The present paper concerns x-ray absorption spectroscopy experiments at the As K-edge on InAs up to 80 GPa. The aim of this study is to obtain quantitative information on the local environment of As in the post-NaCl phases of InAs. These measurements confirm the absence of the CsCl phase, and the analysis of the fine structure of the x-ray absorption allows us to characterize the local structure of the high pressure phases of InAs from their onset of appearance. While the *Cmcm* phase is locally very similar to the NaCl structure, having a first coordination shell of six indium atoms, above 31 GPa an increasing number of As atoms are detected within a distance of 3.16 Å.

1. Introduction

The traditional knowledge of the behaviour under compression of the $A^N B^{(8-N)}$ octet semiconductors is based on the fact that, with pressure, the four-fold coordinated structures with low densities are transformed to denser phases of increased coordination: four-fold (diamond, zincblende, wurtzite) → six-fold (β-Sn, NaCl) → eight-fold (CsCl) [1]. This structural sequence has been confirmed by a large number of experimental and theoretical works up to the end of the 1980s. In the last decade, experiments have shown a systematic absence of the NaCl-type high pressure phases in the more covalent compounds [2, 3] as well as a systematic absence of the β-Sn-type high pressure phases in the more ionic compounds [4]. These new findings have been explained using linear response phonon calculations which take into account phonon instabilities of the high pressure phases [5]. In the higher pressure regime [6], the same method finds that the CsCl phase is dynamically unstable for the more ionic members of $A^N B^{(8-N)}$ octet semiconductors (GaP, GaAs, InP, and InAs), while for the more covalent InSb no phonon instability can prevent the CsCl phase from forming, and a chemically disordered CsCl structure has indeed been observed [7].

[1] Author to whom any correspondence should be addressed.

An important point in the full characterization of the structures of the high pressure phases is their degree of order. A structure is site ordered when each atomic position is occupied by only one atomic species with an integer site occupancy, whereas in a site disordered structure the same atomic position may be occupied by more than one atomic species with a fractional site occupancy. X-ray diffraction (XRD) can address this issue by the presence of the so-called 'difference' reflections [8]. High pressure conditions lead to microstructural effects in the samples that broaden Bragg peaks. Such effects may hide the 'difference' reflections, especially in those compounds where the scattering power of the two atomic species are very similar, like in GaAs, giving rise to an erroneous estimation of the site ordering of the high pressure structures. All previous XRD works on the evolution of InAs with pressure (including our own) have not been conclusive on the issue of site ordering in the high pressure phases [3, 9, 10]. Besides this drawback, the fact that XRD shows that the average structure is site disordered does not exclude the existence of an ordering over a short length range. The information on the short-range order of the structures of the high pressure phases of solids is crucial for the understanding of the fundamental interactions between the atoms in the matter. Reliable information about the short-range order allows us to validate the theoretical methods that yield the formulation of models and interatomic potentials used to reproduce the thermodynamic and structural properties of matter. In this context, x-ray absorption spectroscopy (XAS) can play an important role. In fact, XAS is able to distinguish site order from site disorder within the nearest-neighbour distance from the photoabsorber since it probes selectively its local environment and is sensitive to the nature of the surrounding neighbours.

Indium arsenide is among the more ionic III–V semiconductors and it has the lowest predicted transition pressure to CsCl [11]. We have recently demonstrated that the high pressure NaCl phase of InAs transforms to a *Cmcm* structure in agreement with a previous XRD study of Nelmes *et al* [3], and it undergoes a further phase transition not to a CsCl phase but to a *Pmma* structure [10] that persists at least up to 46 GPa. That result highlighted recent theoretical calculations that found the *Pmma* symmetry to be a direct consequence of a phonon instability of the CsCl structure [6]. Moreover, by a qualitative comparison of the near edge part of the spectra with full multiple scattering calculations we found that the high pressure *Pmma* phase is short-range chemically disordered.

In this paper we present XAS measurements at the As K-edge of InAs up to 80 GPa. The zincblende (ZB) to NaCl phase transition is not discussed, and the relative information can be found in Pascarelli *et al* [12]. To our knowledge these are the first XAS measurements to such high pressures. Such outstanding experimental achievements are possible thanks to the high flux provided by third generation synchrotron sources such as ESRF and to the recent developments in the optics of the dispersive XAS beamline at ESRF, ID24 [13]. This energy-dispersive x-ray absorption spectrometer offers stable and small focal spots of about $10 \times 10\ \mu\text{m}^2$ that are mandatory for such high pressure measurements because of the small sample size.

The aims of this EXAFS (extended x-ray absorption fine structure) work were to obtain quantitative information on the local environment of As in the high pressure phases of InAs, and in particular to carry out the following.

- Check for the presence of As neighbours in the *Cmcm* phase which was qualitatively found to be chemically ordered in our previous XANES (x-ray absorption near edge structure) analysis.
- Check for the presence of As neighbours in the *Pmma* phase and try to establish their number. This phase was found to be chemically disordered in our previous qualitative XANES analysis.

- Check for the presence of the theoretically predicted CsCl phase in the newly explored pressure region up to 80 GPa.

The data show the evidence of three phase transitions in the pressure range of the experiment that, in the light of the previous XRD studies [3, 10, 9], may be identified as ZB $\rightarrow$ NaCl $\rightarrow$ *Cmcm*$\rightarrow$ *Pmma*. The analysis of the EXAFS signal has been performed to give, for the first time, quantitative information on the local environment and therefore on the short-range order around in the high pressure phases of InAs.

The organization of this paper is as follows. In section 2 we describe the experimental details of the XAS measurements. In section 3 we present the data and their evolution as a function of pressure from a qualitative point of view. In section 4 we describe all the crystal structures referred to in the data analysis (CsCl, NaCl, *Cmcm*, and *Pmma*), giving a particular emphasis to the local arrangement of the atoms around As. The details of the data analysis together with the results are presented in section 5. Finally, in section 6 we give several conclusions.

2. Experimental details

The XAS measurements were carried out at the dispersive EXAFS beamline at ESRF, ID24 [13] at the As K-edge (11 867 eV). The InAs sample consisted of a fine powder ground from 99.9999% purity polycrystalline stock (Alfa). The sample was loaded, with a 4:1 mixture of methanol:ethanol as pressure transmitting medium, in a Chervin-type diamond anvil cell [14] fitted with 150 μm bevel-edged diamonds. To contain the sample, a stainless steel gasket was used, with 50 μm diameter hole and an initial thickness of 30 μm. The pressure was measured using the ruby fluorescence method [15]. The data were recorded at room temperature. The maximum pressure reached was 80 GPa and after the first data point at 0.4 GPa the data were collected in a pressure range from 11 to 80 GPa every 6–7 GPa.

The major problem of using a diamond anvil cell to generate the pressure is that, for given energies, the photons are diffracted by the anvils, giving rise to Bragg diffraction peaks in the spectra that are often more intense than EXAFS and XANES oscillations. The energy dispersive set-up allows one to minimize relatively easily the appearance of such strong Bragg peaks in the energy range of interest by following on line the transmitted beam on the two-dimensional detector as a function of the diamond orientation. Nevertheless, the occurrence of Bragg peaks remains the main limit to the energy range of high pressure XAS data and strongly penalizes their exploitation. In this case the Bragg reflections limited the k-range of the spectra to a maximum of 8 Å^{-1}.

3. Qualitative description of data and evolution with pressure

Figure 1(a) shows the As K-edge spectra of InAs and the extracted EXAFS signals $k\chi(k)$ (b). The dramatic change in the oscillations frequency from 0.4 to 11 GPa reflects the different local environment around As when going from a zincblende (ZB) structure with four In first neighbours at 0.4 GPa to an NaCl structure with six In first neighbours at 11 GPa. After that, an overall view of the EXAFS signals shows small modifications, such as the gradual loss of the shoulder at $k \sim 3$ Å^{-1}, a decrease of the main frequency and an overall broadening of the features together with an attenuation of the intensity of the oscillations.

The XANES spectra for some selected pressures are shown in figure 2. Besides the clear modification between 0.4 and 11 GPa corresponding to the ZB $\rightarrow$ NaCl phase transition, the evolution with pressure of the near edge part of the absorption spectra shows quite clearly

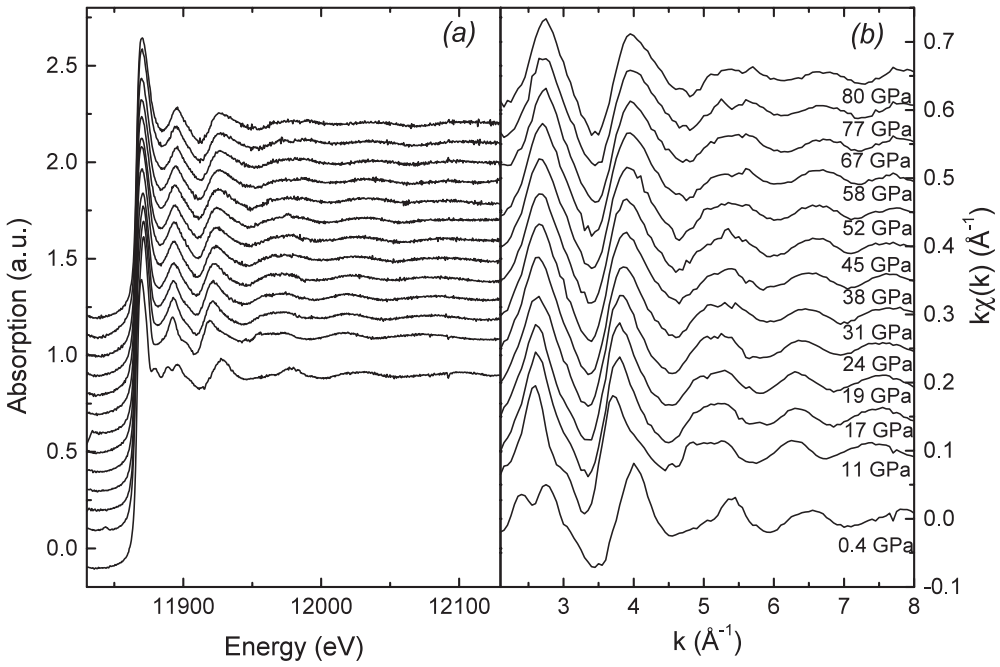

Figure 1. Raw XAS spectra of InAs (a) and relative extracted $k\chi(k)$ (b) from 0.4 to 80 GPa.

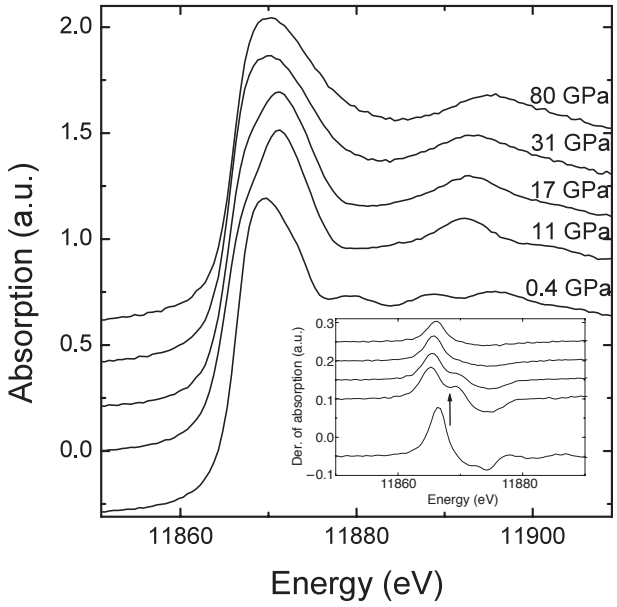

Figure 2. XANES spectra of InAs up to 11 910 eV at 0.4, 11, 17, 31 and 80 GPa. The inset shows the first derivative of the absorption.

modifications also above 11 GPa. The first is at 17 GPa, where the 'triangular' shape of the white line is rather reduced. This modification can be seen more easily in the derivatives of the

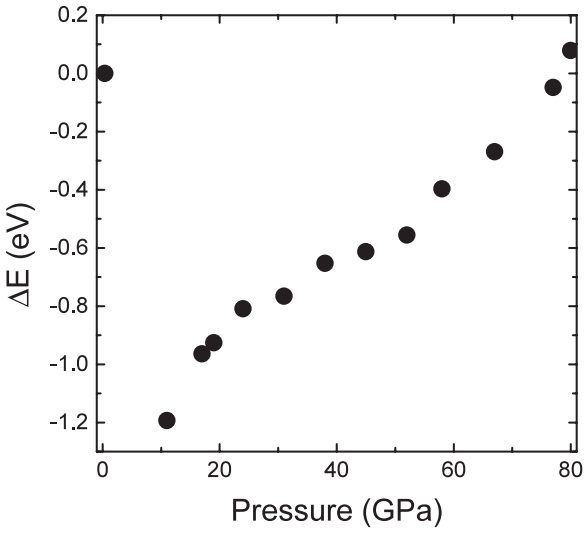

Figure 3. Energy variation of the maximum of derivative of the absorption spectra as a function of pressure.

absorption spectra shown in the inset of figure 2, where the dip to the right of the maximum of the derivative indicated by an arrow is smoothed. The second important modification is at 31 GPa, where the white line becomes rounded with a complete disappearance of the dip in the derivative. We attribute these changes to the onset of two different phase transitions: NaCl $\rightarrow$ *Cmcm* at 17 GPa and *Cmcm* $\rightarrow$ *Pmma* at 31 GPa. The analysis of the position of the maximum of the derivative shown in figure 3 indicates a shift of $-1.2(1)$ eV in the onset of absorption occurring between the four-fold and the six-fold coordinated phases. This highlights that the energy gap between the valence and conduction band has closed and that the electronic structure of the high pressure phase has a metallic character, in agreement with previous findings [16].

The analysis of the Fourier transforms, that is independent from any theoretical model, shows as well modifications at 17 GPa and at 31 GPa. The imaginary parts of the Fourier transforms of the experimental $k\chi(k)$ calculated in a k-range of 2–8 Å^{-1} are plotted in figure 4. If we consider the two maxima A and B around $R \sim 3$ Å, the ratio $A/B \simeq 1$ at 11 GPa (continuous curve). After this pressure point the ratio $A/B > 1$ for 17, 19 and 24 GPa (dashed curves), while in the following curves the ratio $A/B < 1$, and it monotonically decreases with pressure (dotted curves). We will show in the following section that the quantitative analysis of the EXAFS signals attributes these changes in the A/B ratio to the onsets of two different phase transitions: namely to the distortion of the NaCl structure, with the onset of the *Cmcm* phase at 17 GPa, and to the appearance of As atoms as nearest neighbours, with the onset of the *Pmma* phase at 31 GPa. Moreover, the increase of the maximum B with respect to the maximum A is explained as an increase of the number of As atoms approaching the photoabsorber as a function of pressure in the *Pmma* phase.

In a first qualitative analysis of the data we have followed, as a function of pressure, the extracted $k\chi(k)$ signal, the near edge part of the raw absorption spectra, and the imaginary part of the Fourier transform. While no substantial differences can be observed after the ZB $\rightarrow$ NaCl transition in the extended part of the spectra, the behaviour of the near edge and of the Fourier transforms suggests phase transitions at 17 and 31 GPa.

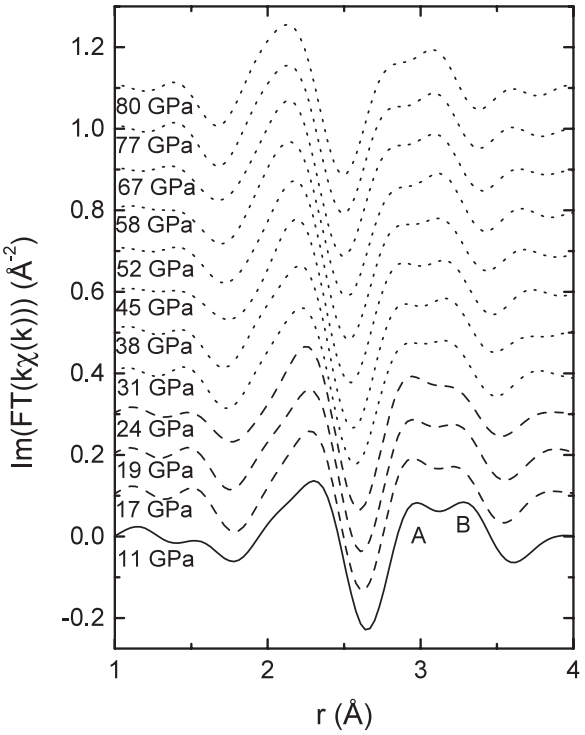

Figure 4. Imaginary part of the Fourier transform as a function of pressure. $A/B \simeq 1$ for the data point at 11 GPa (continuous curve), $A/B > 1$ from 17 to 24 GPa (dashed curves), and $A/B < 1$ from 31 to 80 GPa (dotted curves).

4. Crystal structures

4.1. CsCl

The CsCl structure is sketched in figure 5. It presents well defined coordination shells given by eight atoms as first neighbours and by six atoms as second neighbours. The relationship between the first and the second neighbour distances R^{1st} and R^{2nd} is given by $R^{2nd} = 2/\sqrt{3}R^{1st}$.

4.2. NaCl

The NaCl structure is sketched in figure 6. It presents well defined coordination shells given by six atoms for the first and twelve for the second. The relationship between the first and the second neighbour distances R^{1st} and R^{2nd} is given by $R^{2nd} = \sqrt{2}R^{1st}$.

4.3. Cmcm

The *Cmcm* structure, sketched in figure 7(a), can be seen as an orthorhombic distortion of the NaCl structure. It has two atomic positions at (0, y_1, 1/4) and (0, y_2, 1/4). If $a = b = c$ and $y_1 = 3/4$ and $y_2 = 1/4$, then the structure is identical to NaCl. The two distortions from NaCl are a shift of the x–y planes along the y direction and a smaller zigzag distortion along the x direction that arises when $\Delta y = y_1 - y_2 \neq 1/2$. Such distortions make the atomic

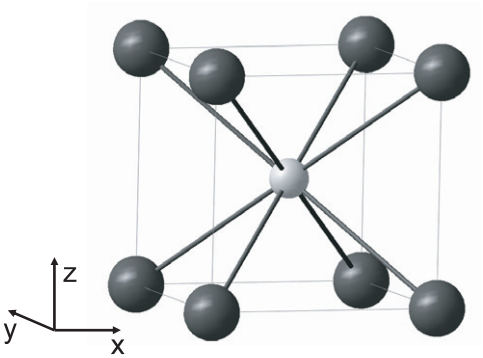

Figure 5. CsCl structure. The As atom (white atom) is surrounded by eight In atoms (grey atoms).

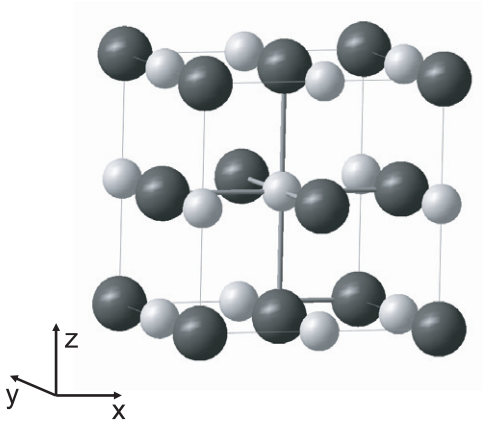

Figure 6. NaCl structure. The As atom (white atom) is surrounded by six In atoms (grey atoms).

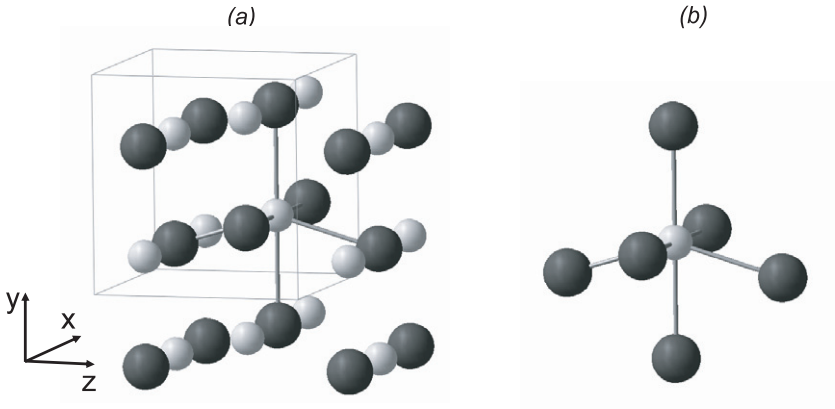

Figure 7. (a) *Cmcm* structure of InAs. $a = 5.2625$ Å, $b = 5.4313$ Å, $c = 5.1996$ Å. In is at (0, 0.6792, 0.25) and As is at (0, 0.1797, 0.25). Since $\Delta y = y_1 - y_2 \simeq 1/2$ the zigzag distortion along the x axis is small. These structural parameters have been obtained at 25 GPa from full Rietveld refinement of XRD data [10]. (b) Split-distance first neighbour shell of six In atoms (grey atoms) around As (white atom) of InAs in the *Cmcm* structure.

cluster around the photoabsorber atom to be no longer formed by a first neighbour single distance shell of six atoms like in the NaCl structure. As the degree of the distortion increases (with pressure application for instance), the first single distance shell of six atoms splits into different *sub-shells* (but at similar distances) of one or two atoms. The structure in figure 7(a) corresponds to the structural parameters obtained from a full Rietveld refinement at 25 GPa which was the last XRD data point before the onset of the post-*Cmcm* phase. At this pressure the local environment of As (figure 7(b)) is still given by six In, but at four different distances between 2.63 and 2.72 Å.

4.4. Pmma

The *Pmma* structure, sketched in figure 8(a), has been found in InAs as a post-*Cmcm* phase [10]. It is a subgroup of *Cmcm* with the loss of the *C*-centering condition. The transformation from

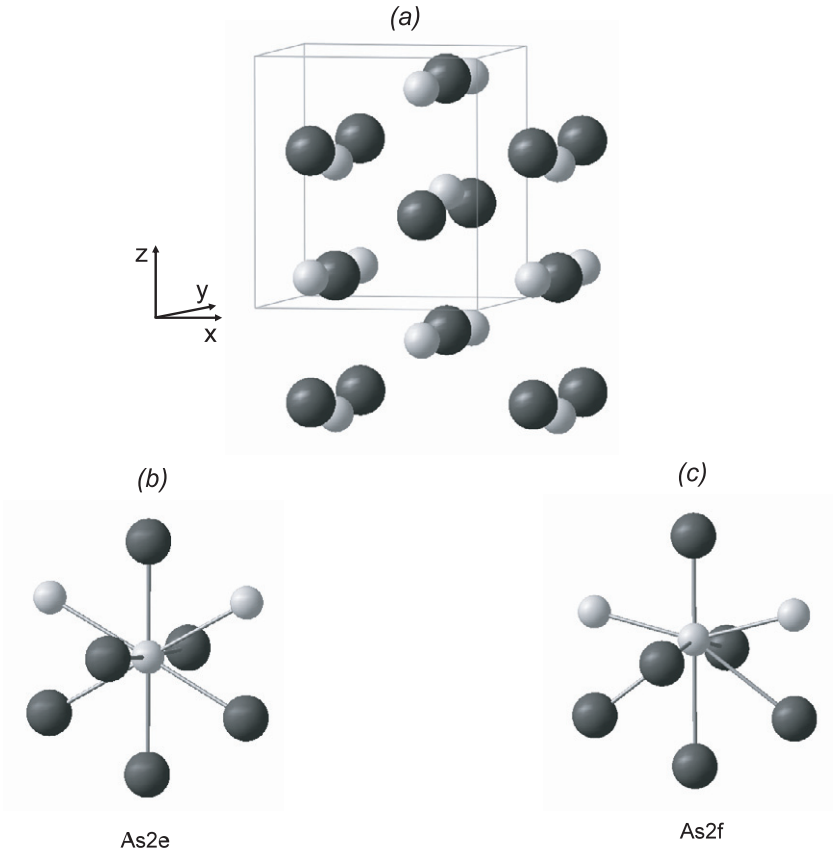

Figure 8. (a): *Pmma* structure of InAs at 45 GPa. $a = 4.8931$ Å, $b = 5.1069$ Å, $c = 5.4117$ Å [In 2e: 0.75, 0, 0.3735], [As 2e: 0.75, 0, 0.8776], [In 2f: 0.25, 0.5, 0.1065], [As 2f: 0.25, 0.5, 0.557]. (b) and (c): The local environment of As (white atom) in InAs in the *Pmma* structure when the photoabsorber is in the As 2e and As 2f positions, respectively.

Cmcm to *Pmma* follows from the splitting of the 4c positions of *Cmcm* into 2e and 2f positions of *Pmma*. The structure in figure 8(a) corresponds to the structural parameters obtained from a full Rietveld refinement at 45 GPa [10]. The local environment of As in InAs in the *Pmma* structure, as derived from the Rietveld analysis, is sketched in figure 8 when the photoabsorber is in the As 2e (b) and in the As 2f (c) positions.

The sketches show that two As neighbours are present in either case, embedded in the In neighbours. However, it is worth recalling that the Rietveld analysis was unable to be conclusive on the fraction of occupancy of each species on the 2e and 2f sites, since refinements based on models with different occupancies yielded statistically equivalent fits.

5. EXAFS data analysis

5.1. Introduction

The EXAFS data analysis was carried out using the codes from the UWXAFS package [17]. Phase shifts for photoabsorber and backscatterer atoms were calculated by FEFF8 [18] using a self-consistent energy dependent exchange correlation Hedin–Lundqvist potential. Structural

Table 1. First-shell parameters determined by XAS data analysis as a function of pressure.

P (GPa)	$R_{\mathrm{As-In}}$ (Å)	$\sigma^2_{\mathrm{As-In}}$ (Å^2)
11	2.73(1)	0.014(3)
17	2.70(1)	0.012(2)
19	2.69(1)	0.012(2)
24	2.68(1)	0.013(1)

data for the high pressure phases used by the ATOMS program [19] to prepare the input for FEFF8 were taken from the Rietveld refinement of our XRD data [20].

The experimental XAFS, $\chi(k)$, was obtained after subtracting the embedded-atom absorption background from the measured absorption coefficient [21] and normalizing by the edge step. XAFS data were Fourier transformed to real space and fitted in the range $\Delta R \simeq 1.2$–3.2 Å.

5.2. Low pressure

The data from 11 up to 24 GPa were fitted using a theoretical model obtained from an NaCl structure. It is worth recalling that the 'discontinuity' observed in the evolution of the shape of the near edge at 17 GPa has been attributed to the NaCl $\rightarrow$ *Cmcm* transition. In the limit of small deviations from the NaCl structure and considering the k-range of the EXAFS data, the data corresponding to the *Cmcm* phase could be fitted with an NaCl model using a single distance shell. The results of the fitting for the first coordination shell between 11 and 24 GPa are reported in table 1. The gradual splitting of the first shell distance into several different (but close) distances as pressure increases should be seen through a gradual increase in the bond length variance, $\sigma^2_{\mathrm{As-In}}$, associated to thermal and static configurational disorder in this shell. It is well known [22–24] that the effect of pressure is to reduce thermal disorder, so the observation of a constant value of $\sigma^2_{\mathrm{As-In}}$ between 11 and 24 GPa is a clear indication of the increasing static disorder of the *Cmcm* phase with respect to the model NaCl phase. Figure 9 shows the comparison between the experimental EXAFS function $\chi(k)$ for the data at 17 GPa and the theoretical best-fit results. The residual function (bottom curve of figure 9) contains the frequencies associated to higher distance shells and to multiple scattering contributions. This is to be expected since our fits are limited to the region $\Delta R \simeq 1.2$–3.2 Å. All frequencies corresponding to paths above 3.2 Å are excluded from our fitting model.

5.3. High pressure

The same model has been tested to fit the data from 31 up to 80 GPa. The best-fit calculations compared with the experimental EXAFS spectrum for the data at 52 GPa are shown in figure 10. Starting from the data at 31 GPa, the fit is poor and gets worse with increasing pressure. The residual function shows a well defined oscillatory behaviour along the whole k-range and therefore cannot be attributed only to the absence in the fit of longer paths. The bad modelling of the nearest neighbours environment given by the NaCl structure gives an important contribution to the misfit. The first attempted model alternative to the NaCl model is based on the CsCl structure. The theoretical phase shifts have been calculated for a CsCl structure whose density at 45 GPa is equivalent to that obtained from the refinement of the XRD data reported in [10]: i.e. 9.32 g cm^{-3}. With this assumption the first shell of eight In atoms is at a distance of 2.80 Å and the second shell of six As atoms is at 3.23 Å. All the data above 31 GPa have been fitted using this model considering both the first shell only ($\Delta R \simeq 1.2$–3.2 Å) and the

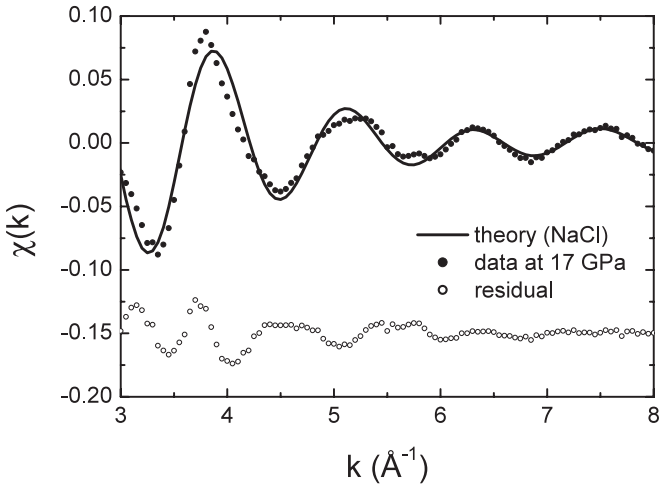

Figure 9. Comparison between the experimental EXAFS spectrum at 17 GPa (dots) and the best-fit calculation (solid curve) corresponding to a single-distance shell of six In atoms. The bottom curve shows the residual function.

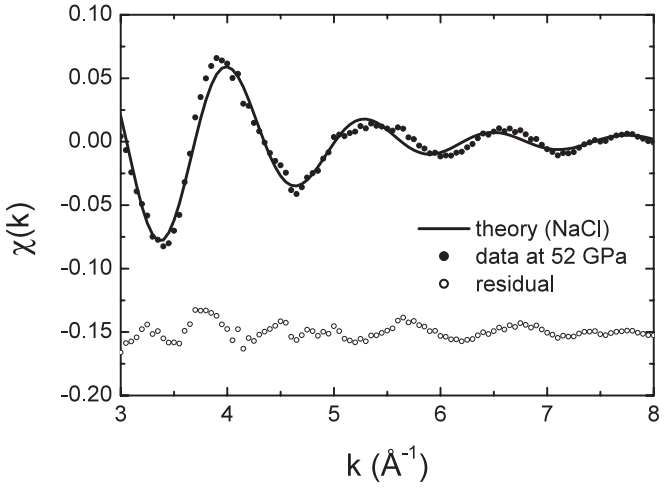

Figure 10. Comparison between the experimental EXAFS spectrum at 52 GPa (dots) and the best-fit calculation (solid curve) corresponding to a single-distance shell of six In atoms. The bottom curve represents the residual function.

first and second shells ($\Delta R \simeq 1.2$–3.7 Å). For the fits including the first two shells the second shell distance was linked to the first shell one according to the relationship between the first and the second neighbour distance in the CsCl structure. In figure 11 we report, from top to bottom, the best-fit calculations corresponding to the As–In and As–As scattering, the total signal superimposed on the experimental EXAFS $\chi(k)$ and the residual function. The misfit using the CsCl structural model is similar to that observed using the NaCl model. This is due to the fact that during the fit procedure the Debye–Waller factor relative to the As–As scattering diverges, flattening its contribution and becoming irrelevant to the fit. Constraining the $\sigma^2_{\mathrm{As-As}}$ to vary between certain limits does not improve the quality of the fit.

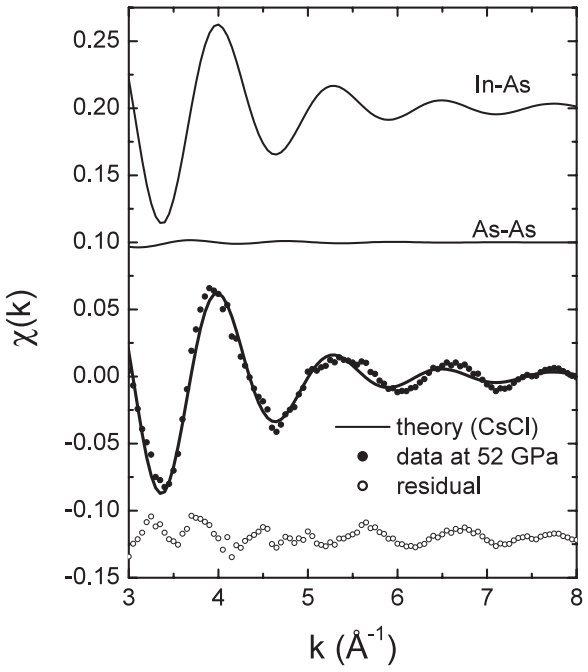

Figure 11. *Solid curves*: From top to bottom, best-fit calculations corresponding to the In–As, As–As, total signal and residual. The total signal is directly compared to the experimental EXAFS function (dots).

For the data above 31 GPa the models based on a local environment of six In atoms and based on a CsCl structure were therefore excluded, and a different structural model had to be found. In observing the residual function of the model based on six In atoms, we noticed that it contained the frequency corresponding to an As contribution at a distance of 3.16 Å that decreased down to 3.10 Å at 80 GPa. However, because of the well known problem of the high correlation between the coordination number and the Debye–Waller-like factor [25], it was impossible to be conclusive on the number of As atoms approaching the first six In atoms and the $\sigma^2_{\mathrm{As-As}}$ without making additional assumptions on the structure. A lower limit for N_{As} can be estimated by fixing $\sigma^2_{\mathrm{As-As}}$ to a lower limit value given by that associated to the closer As–In bonds, i.e. 0.013 Å^2. We performed a set of fits leaving the number of As–As bonds as a free parameter and fixing the $\sigma^2_{\mathrm{As-As}}$. Figure 12 shows the comparison between the experimental EXAFS function for the data at 52 GPa and the theoretical best fit results and the single As–In and As–As contributions. The residual function exceeds the noise level only at low k. This is due to higher shells and to multiple scattering contributions, whereas the good agreement at high k indicates that the model describing the near environment given by six In and four As atoms is correct. Table 2 shows the structural parameters that reproduce the experimental data from 31 to 80 GPa. This table shows that a non-negligible contribution of As atoms, whose coordination number increases with pressure, is observed in addition to six In atoms.

Let us return to the behaviour of the Fourier transform discussed in section 3. Figure 13 reports the imaginary part of the Fourier transforms relative to the As–In (dotted curve) and the As–As (dashed curve) contributions to the fit at 52 GPa (solid curve). The As–As signal is negligible with respect to that of As–In except in the zone highlighted by the box. In that

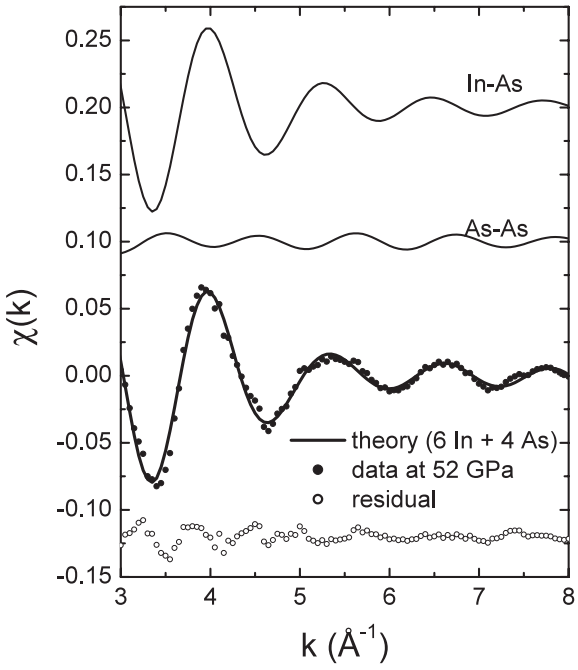

Figure 12. *Solid curves*: From top to bottom, best-fit calculations corresponding to the In–As, As–As, total signal and residual. The total signal is directly compared to the experimental EXAFS function (dots).

Table 2. Structural parameters determined by XAS analysis for data from 31 up to 80 GPa.

P (GPa)	$R_{\mathrm{As-In}}$ (Å)	$\sigma^2_{\mathrm{As-In}}$(Å^2)	$R_{\mathrm{As-As}}$ (Å)	N_{As}
31	2.66(1)	0.013(3)	3.16(5)	3(2)
38	2.64(1)	0.013(2)	3.16(6)	3(2)
45	2.63(1)	0.014(2)	3.16(4)	4(2)
52	2.62(1)	0.014(2)	3.13(3)	4(2)
58	2.61(1)	0.016(3)	3.11(4)	4(2)
67	2.59(1)	0.016(2)	3.11(4)	4(1)
77	2.59(2)	0.016(3)	3.11(4)	4(2)
80	2.59(2)	0.017(3)	3.10(5)	4(3)

region the As–As contribution is in antiphase with the As–In signal, lowering the maximum due to the As–In signal at 2.9 Å and introducing the shoulder at 3.1 Å. This is exactly the effect seen and discussed in section 3 on the imaginary part of the Fourier transforms of figure 4. With increasing coordination of As the shoulder at 3.1 Å increases to the detriment of the maximum at 2.9 Å. From this argument and assuming a criterion that breaks the correlation between the Debye–Waller-like factor and the coordination number, it follows that the As coordination increases with pressure. We emphasize that the number of As–As bonds arising from the fitting procedure is to be considered as a lower limit. The local environment of As above 31 GPa is compatible with a *Pmma* structure as determined by XRD [10]. However, the measured coordination of As using a local and direct method, such as EXAFS, is higher than that present in the structure shown in figures 8(b), (c).

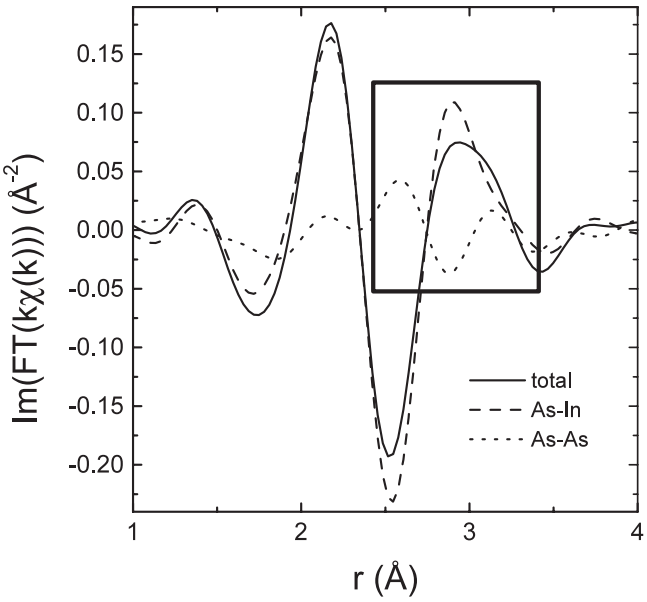

Figure 13. Imaginary part of the Fourier transform corresponding the As–In scattering (*dotted curve*) and to the As–As scattering (*dashed curve*). The continuous curve is the sum of the two contributions.

6. Conclusions

In conclusion, we performed an XAS experiment at the As K-edge on InAs up to 80 GPa showing the first XAS measurements to such high pressures. The data recorded after the ZB → NaCl phase transition, in particular the near edge part of the spectra and the analysis of the Fourier transform, show that InAs undergoes two phase transitions in the range of pressure in which the experiment has been done. The first, at 17 GPa, is attributed to the NaCl → *Cmcm* phase transition, and the second, at 31 GPa, to the *Cmcm* → *Pmma* transformation. The analysis of the data proves that InAs in the *Cmcm* phase can be described locally by an NaCl environment given by six In atoms with an increased degree of static disorder given by a pressure increasing Debye–Waller-like factor. That is to say that the local environment of As in InAs in the *Cmcm* structure is chemically ordered and no short-range As–As interactions are present in the *Cmcm* phase. This result is in agreement with our previous qualitative XANES analysis. At 31 GPa this model does not describe the data nor does a model based on a CsCl structure with eight In atoms as first neighbours. The local environment of InAs in the *Pmma* phase that best describes the data is given by six In neighbours, followed closely by As neighbours. The minimum number of As neighbours approaching the In neighbours increases with pressure, indicating that the As–As interactions in InAs at high pressure are more likely to occur than would be expected from a *Pmma* phase as obtained from XRD. Therefore, InAs at high pressure presents a local environment around As that is chemically disordered. This confirms quantitatively our previous qualitative analysis of the XANES spectra with a multiple scattering calculation. These results show that EXAFS spectroscopy is able to give a valuable insight into the local structure, yielding information on the chemical ordering of high pressure phases that is very complementary to XRD to fully characterize high pressure structure in solids.

Acknowledgment

We would like to thank Sebastien Pasternak (ESRF) for his invaluable technical support during the experiment.

References

[1] Phillips J C 1973 *Bond and Bands in Semiconductors* (New York: Academic)
[2] McMahon M I and Nelmes R J 1995 *J. Phys. Chem. Solids* **56** 485
[3] Nelmes R J, McMahon M I, Wright N G, Allan D R, Liu H and Loveday J S 1995 *J. Phys. Chem. Solids* **56** 539
[4] Nelmes R J, McMahon M I and Belmonte S A 1997 *Phys. Rev. Lett.* **79** 3668
[5] Ozoliņš V and Zunger A 1999 *Phys. Rev. Lett.* **82** 767
[6] Kim K, Ozoliņš V and Zunger A 1999 *Phys. Rev.* B **60** 8449
[7] Vanderborgh C A, Vohra Y K and Ruoff A L 1989 *Phys. Rev.* B **40** 12450
[8] Nelmes R J and McMahon M I 1998 *Semiconductors and Semimetals* vol 54 (London: Academic) p 145
[9] Aquilanti G, Crichton W A, Le Bihan T and Pascarelli S 2003 *Nucl. Instrum. Methods* B **200** 90
[10] Pascarelli S, Aquilanti G, Crichton W A, Le Bihan T, Mezouar M, De Panfilis S, Itié J-P and Polian A 2003 *Europhys. Lett.* **61** 554
[11] Mujica A and Needs R J 1997 *Phys. Rev.* B **55** 9659
[12] Pascarelli S, Aquilanti G, Crichton W, Le Bihan T, De Panfilis S, Fabiani E, Mezouar M, Itié J-P and Polian A 2002 *High Pressure Res.* **22** 331
[13] Pascarelli S, Mathon O and Aquilanti G 2004 *J. Alloys Compounds* **362** 33
[14] Chervin J C, Canny B, Besson J M and Pruzan Ph 1995 *Rev. Sci. Instrum.* **66** 2595
[15] Forman R A, Piermarini G J, Barnett J D and Block S 1972 *Science* **176** 284
[16] Minomura S and Drickamer H G 1962 *J. Phys. Chem. Solids* **23** 451
[17] Stern E A, Newville M, Ravel B, Yacoby Y and Haskel D 1995 *Physica* B **208/209** 117
[18] Ankudinov A L, Ravel B, Rehr J J and Conradson S D 1998 *Phys. Rev.* B **58** 7565
[19] Ravel B 2001 *J. Synchrotron Radiat.* **8** 314
[20] Aquilanti G 2002 *PhD Thesis* University J Fourier, Grenoble, France
[21] Newville M, L̄iviņš P, Yacoby Y, Rehr J J and Stern E A 1993 *Phys. Rev.* B **47** 14126
[22] Di Cicco A, Filipponi A, Itié J-P and Polian A 1996 *Phys. Rev.* B **54** 9086
[23] Yoshiasa A, Nagai T, Ohtaka O, Kamishima O and Shimomura O 1999 *J. Synchrotron Radiat.* **6** 43
[24] Comez L, Di Cicco A, Itié J-P and Polian A 2001 *Phys. Rev.* B **65** 14114
[25] Koningsberger D C and Prins R 1988 *X-ray Absorption: Principles, Applications, Techniques of EXAFS, SEXAFS, and XANES* (New York: Wiley)